Simulation of the binaural environmental transfer function for gerbils using a boundary element method

Sheryl M. Grace, Erika Quaranta, [a)]
Aerospace and Mechanical Engineering Department

Barbara G. Shinn-Cunningham,
Cognitive and Neural Systems Department

and

Herbert F. Voigt
Biomedical Engineering Department
Boston University, 110 Cummington St., Boston, MA 02215

(September 21, 2007)

Running title: Gerbil binaural environmental transfer function simulation

---

[a)] Electronic mail: sgrace@bu.edu

1

ABSTRACT

The auditory system relies on spectral notches in the binaural environmental transfer function (BETF) as cues for localization of sources in the median plane. Experiments have shown that the BETF for gerbils in free space, regularly termed the head related transfer function (HRTF), contains a single notch in the ultrasonic range, while the BETF for a gerbil standing on a solid surface contains several notches at much lower frequency due to comb-filtering effects. In this research, the BETF for a model gerbil geometry is computed using a boundary element method (BEM). A parallel implementation of the BEM that includes the CHIEF regularization scheme is applied. The gerbil's BETFs for various source elevations and distances in the free-field and in the presence of a solid surface are computed. Comparisons with gerbil HRTF measurements show good agreement. The reflection due to the solid surface is shown to provide an acoustic cue for source elevation as well as source distance. It is demonstrated that the full variation of the BETF with source location can only be captured through a simulation that can account for both the solid surface and the gerbil and their combined influence on the sound field.

PACS numbers: 43:66Qp, 43:64Bt, 43:64Ha.

1. INTRODUCTION

Spatial perception of sound contributes to the ability of humans and animals to produce a mental picture of their surrounding environment. It is known that the head and especially the pinna (outer ear) modify incident sound waves by attenuating or amplifying them, in a frequency dependent manner, before they reach the eardrum (Blauert, 1993). In particular, the pinna geometry often significantly attenuates the sound at some frequency, causing a spectral notch. In addition, the environmental setting plays a role in altering the sound waves that arrive at the ear.

Interaural time and intensity cues provide robust information about the location of a source relative to the interaural axis. However, these interaural differences are not useful for determining the location relative to the up/down directions. Instead, spectral cues, which vary with the elevation of the sound relative to the ear, are the primary cue for disambiguating location within a so-called "cone of confusion." It is thought that spectral notches, filtered out of the broadband signals by the pinna, are the cues used in this case, because the frequency at which the spectral notch occurs has been shown to be a function of elevation Raykar *et al.* (2005).

The filter function for an isolated head that relates the transformation of the acoustic signal by the filtering action of the pinna is known as the Head-related Transfer Function (HRTF). When one considers the effect of the body and environmental obstacles, the appropriate transfer function better labeled as the Binaural Environmental Transfer Function (BETF).

It is most common to find measurements of HRTFs in the literature. In particular,

the HRTF of humans is reported in (Blauert, 1993), the monkey's HRTF is reported in (Spezio *et al.*, 2000), gerbil HRTF's can be found in Maki *et al.* (2003a), and several researchers have measured the HRTF for cats (Musicant *et al.*, 1990; Rice *et al.*, 1992; Xu and Middlebrooks, 1980; Young *et al.*, 1996). Some BETF measurements have been made in an attempt to extract the effect of environment on human hearing (Rakerd and Hartmann, 1985; Shinn-Cunningham *et al.*, 2005). Recently, a study of the BETF for gerbils was completed by Maki *et al* (2003b; 2005).

Studies on the physiology of gerbil hearing have shown that the neurons in the dorsal cochlear nucleus (DCN), which are known to act as spectral notch detectors (Parsons *et al.*, 2001; Spirou and Young, 1991; Young *et al.*, 1992), have excitatory responses to best-frequency (BF) tones as low as $1 \, kHz$ (Parsons *et al.*, 2001). The question of why the DCN would have this low frequency sensitivity when the spectral notch in the gerbil HRTF occurs at high frequency was partially resolved by the BETF studies carried out by Maki *et al* (2003a; 2005). They showed that the spectral notches that appear when a gerbil stands on a solid surface occur at low frequencies due to the comb-filtering of the sound field produced by reflections from the floor. They concluded that the surface related cues (as well as posture-related cues) override interaural and spectral cues that have been observed in traditional free-field conditions.

In this research a boundary element method based simulation is used to predict the gerbil BETF in both the free-field and in the presence of a floor for sources in the median plane. The computational results are validated against free-field HRTF measurements. Further computation of the BETF for a gerbil in a simplified envi-

ronment are qualitatively compared to experimental results and are used to explore more deeply the possible importance of various anatomical and geometric features in the presence of a reflecting ground plane.

Two pinna geometries are considered and various pinna base measurement areas are used when computing the HRTF and BETF. Additionally, two definitions of the BETF are compared in this research. First, the ratio of the pressure at the base of the pinna to the pressure at this location when the listener and environmental obstacles are absent is considered. Second, the ratio of the pressure at the base of the pinna to the pressure at this location when the listener is absent but the environmental obstacles are present is considered. These different normalizations help highlight the role of the gerbil geometry in the development of the low frequency notch pattern when the surface is present, especially through the comparison of BETF's for several source locations that produce the same incident pressure field at the gerbil ear due to comb filtering.

In that the results presented agree with the experimental findings of (Maki and Furukawa, 2005), they highlight the utility of a 1 kHz BF tone in the DCN of the gerbil and they support the hypothesis that some animals rely on reflected energy to convey spatial information, such that listening to real or simulated sources in an anechoic environment is not only unnatural, but deprives the listener of information that they expect in order to locate sound sources accurately in their natural environment.

The next section will describe related research that has focused on the computation of the human HRTF and the experimental characterization of the gerbil BETF. The method section describes the boundary element method used for the simulations

shown in this paper. Finally, the results are discussed.

2. BACKGROUND: Modeling HRTFs

The boundary element method has been used extensively in HRTF modeling. Katz (1998), (Katz, 2001a), (Katz, 2001b), Otani and Ise (2003), and Kahana (2000), all used the BEM to compute HRTFs for the human. In these studies the head and pinna shapes were modeled exactly. The studies showed that the computational grids with ten points per wavelength accurately predicted the HRTF. These studies do not indicate that additional features such as a torso or an environmental obstacle can be added easily due to the limit on grid size and computational time. Fels *et al.* (2004) did include the torso while only using 6 points per wave at the higher frequencies. Naka (2006) included environmental obstacles in that a human model was simulated as in a rectangular room with perfectly reflecting walls. The human model however was created using a cube and a cuboid as the head and torso respectively.

Here a single surface reflection is of interest and the focus is on gerbil hearing as opposed to human hearing. Experimental results imply that when environmental cues are present, the detail of the pinna geometry becomes less important. Thus, the present work uses an anatomical model less complicated than many previous studies but more complex than Naka (2006). The ground plane is simulated and the waves are resolved using at least 10 points per wave.

3. METHOD

As mentioned in the previous section, BEM has been used to predict the human HRTF for frequencies below 5-10 kHz. The gerbil free-field spectral notch occurs between 20-40 kHz, but the related nondimensional frequency is similar to that of interest for human hearing. The nondimensional frequency k_{ND} is defined as

$$k_{ND} = \frac{2\pi f a}{c},\tag{1}$$

where c is the speed of sound and a is the meaningful length. The gerbil and human ear length scales are 0.013 m and 0.06 m respectively. For humans then $f = 5kHz$ corresponds to a nondimensional frequency k_{ND} of about 5.5. The same k_{ND} translates to a frequency of roughly 23 kHz for a gerbil.

A zeroth order Boundary Element Method (BEM) formulated in terms of the velocity potential as described in Iemma(2000) is used in this research together with the CHIEF (Combined Helmholtz Interior Integral Equation Formulation) method for damping the effect of spurious roots.

The CHIEF method is easy to implement but its efficiency is strongly dependent on the choice of the interior collocation points $\mathbf{x_i}$. In this research, the CHIEF points were chosen so that they were located close to the maxima of the scattered velocity potential in the interior that appear when no regularization technique is used.

3.1. Implementation

The application of the BEM for simulation of the gerbil BETF is computationally intensive. The frequency range of interest spans from 0.5 to 40 kHz. To obtain a

surface discretization that has at least 10 points per wave length, the surface panels must be on the order of 0.8 mm in each dimension. The gerbil length is on the order of 100 mm, which means that the number of grid points easily reaches 20000 points. Thus at least a 20000×20000 matrix must be stored and solved.

Therefore, a parallel implementation was developed that incorporated MPI (Message Passing Interface) (Snir *et al.*, 1995) and the ScaLAPACK parallel library (Blackford *et al.*, 1997) was used to find the least square error solution. The global matrices were never created, only the form of the local matrices needed on the processing grid were set up, which greatly reduced the memory requirements. The code was run primarily on an Intel Pentium III linux cluster with 1GB of memory and 2 levels of cache on each node.

The model gerbil geometry is symmetric with respect to the median plane. The source locations of interest for this study are located in the median plane. As such, symmetry was also used to reduce the size of the matrix. The entire body was still discretized, and the influence of all of the panels was incorporated into the integral coefficients; however, only half of the collocation points were used. The boundary element code was validated against the analytical solution for scattering from a sphere Quaranta (2004).

4. RESULTS

The BETF is the ratio between the acoustic pressure at the base of the pinna and the acoustic pressure at the ear location when the listener is absent. It is reported in

dB, hence

$$BETF = 20\,Log\left(\frac{\hat{p}}{p^I}\right),\tag{1}$$

where $\hat{p}$ is the amplitude of the total pressure and p^I the incident pressure. The incident pressure p^I originates from a tonal point source of strength Q_S with radial frequency ω, located at a distance r from the ear location. It is expressed as

$$p^I = Q_S\frac{i\omega\rho}{4\pi r}e^{-i\omega r/c}.\tag{2}$$

with the quantity $Q_S \times \rho$ fixed as 1 for all of the simulations reported in this paper. The total pressure, $\hat{p}$, is the summation of the computationally determined scattered and analytically defined incident pressures.

The gerbil geometry was built as a parametric model with no emphasis being placed on a complete anatomical description (i.e. no MRI scans were used to create the model). It consisted of an elliptical ear shape, an ellipsoidal head, and an ellipsoidal torso, as shown in Figure 1. The geometry was parameterized according to data described in (Maki and Furukawa, 2005). The final geometry data for our model is given in Table I.

The gerbil is modeled as acoustically rigid, even though gerbil fur is undoubtedly absorptive. The effect of incorporating absorption into the model would be to attenuate energy reflected off the gerbil body thus decreasing the influence of the body reflections on the results. The results obtained using the rigid-body gerbil are shown in this paper to agree reasonably well with the experimental data and as such justify the assumption that the energy reflected off the gerbil body have a modest influence on the acoustic features of interest here.

TABLE I. Model geometry specs.

Ear		
Length	0.013 m	0.013 m
Width	0.004 m	0.004 m
Depth	0.006 m	0.004 m
Inclination	20°	20°
Distance btw Ears	0.02 m	0.02 m

Head	
Length	0.033 m
Radius (X dir)	0.012 m
Radius (Z dir)	0.010 m

Torso	
Height	0.088 m
Radius (X dir)	0.025 m
Radius (Y dir)	0.020 m
Inclination	60°

Floor	
Distance from Ear	0.095 m
Width	0.4 m × 0.4 m
Thickness	0.001 m
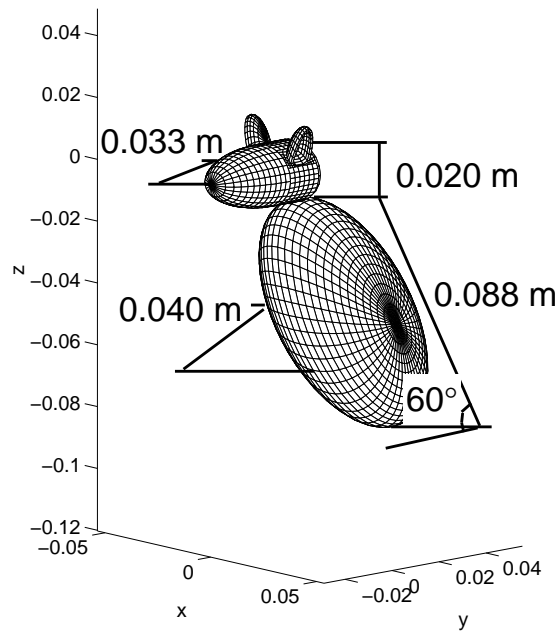
FIG. 1. Gerbil geometry.

Two discretizations of the gerbil geometry were used. A coarser mesh was used

to compute the BETF at lower frequencies while a finer mesh was used for the higher

frequencies. Table II contains the characteristics of the meshes for the gerbil geometry

that includes what will be noted as the first ear shape. At all frequencies, there are

at least 15 panels per wave length on the head and 10 on the torso and on the floor.

This translated to an ear discretization with $(dx, dy, dz) = (0.6, 0.3, 0.7)$ mm for the

coarser grid and $(0.4, 0.2, 0.5)$ mm for the denser grid. This level of discretization was

determined to be adequate through grid resolution studies. For the full gerbil/floor

simulation, the calculation of the transfer function at a single frequency for a single

source using 16 processors on the linux cluster takes up to 40 minutes for the largest

grid. However, in the current BEM formulation, the matrices that must be inverted

are frequency independent so that subsequent frequencies computed for the same

11

TABLE II. Geometry Discretization. Number of Panels.

	Low Frequency 0.5 − 14 kHz	High Frequency 14 − 40 kHz
First Ear	2390	5494
Head	4860	11016
Torso	6400	10000
Floor (top)	14400	N/A

grid and same source location take only 15 minutes. Thus a complete run for a single source location using 120 frequencies takes approximately 30 hours.

The following questions were addressed:

- How sensitive is the computed BETF to the choice of measurement location at the base of the pinna?

- How sensitive is the computed BETF to ear geometry, and is this consistent across experiments?

- How do the computed results compare with the experimental data?

- Can the effect of environmental cues on the BETF be captured by a BEM simulation? If so, what can we learn from the simulations regarding the importance of such cues on perception?

- Can physical insights be gained by choosing different definitions of the incident field when computing the BETF?
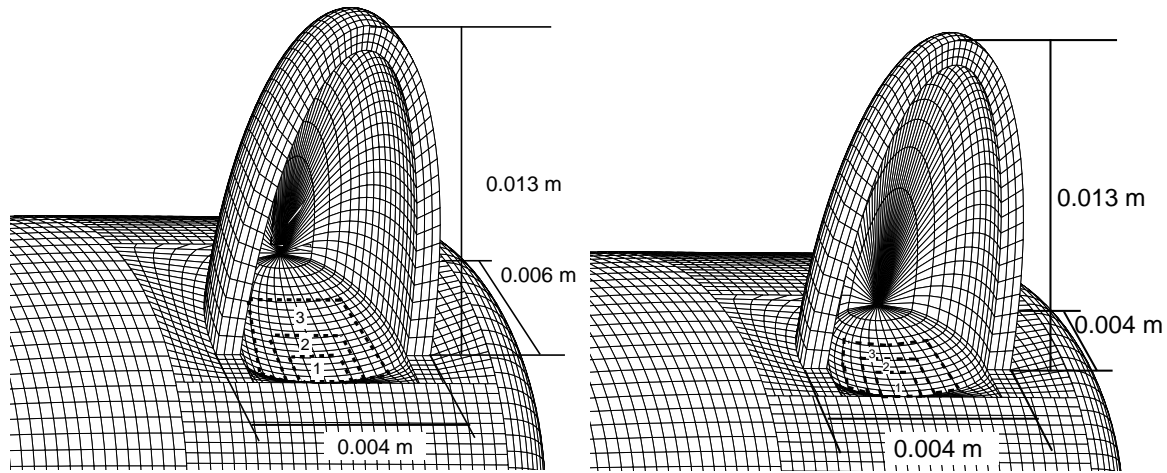
(a) First ear geometry.   (b) Second ear geometry.

FIG. 2. Three areas for BETF average shown.

4.1. Sensitivity to measurement location and ear geometry

Analysis showed that the pressure at the base of the pinna is not uniform and thus the computed BETF, in particular the pinna notch frequency and depth, depends upon the grid point selected for analysis. To minimize the dependence of the BETF on the selected measurement location, the average value of the pressure over a small region at the base of the pinna is used. This choice, of computing a spatial average for the reference pressure, makes the results more directly comparable to results from empirical experiments which use a small microphone or orifice to obtain pressure data. These devices effectively take an average across their measurement membrane. The use of averaging reduced the dependence of the BETF on measurement location, but did not completely remove it.

Figure 2 show two ear geometries studied and three areas over which the pressure

at the base of the pinna was averaged. Area 3 includes area 2, and area 2 includes area 1. Figure 3 shows the effect on the BETF of the area for the first ear model. Two source elevation cases were considered. In both, the source was located 0.3 m from the gerbil head and no torso was present in the model. When no environmental cues and no torso are present, the BETF is exactly the HRTF. The HRTF from the "area 3" average contains three minima of about the same depth. On the other hand, in the HRTF obtained by averaging over "area 1," a single minimum (at 21 kHz) was evident. Moreover, the depths and extent of the minima changed with averaging area. It is in the smallest area case that the excursion of the minimum is greater than 10 dB (a depth that should be easily detectable by the gerbil). When the source was placed at +30° elevation (Figure 3b), the effect of the area choice was still present. From these results, one sees that when a large pinna area is chosen for averaging, some information is lost.

The second ear geometry is slightly less deep than the first ear. The small difference in geometry has a remarkable effect on the HRTF, as shown in Figure 4. At 0° source elevation, the HRTF is only slightly dependent upon the averaging area, and a double notch pattern (that is often seen in the experimental data) appears ($\sim 27\ kHz$). For 30° source elevation, the HRTF does not depend on the averaging area at all. For the first ear geometry, the notch frequency ($\sim 21\ kHz$) corresponds to a wavelength 2.7 times the ear depth and for the second ear geometry, the notch frequency ($\sim 27\ kHz$) corresponds to 3.1 times the ear depth. This similarity in wavelength vs. depth should lead to similar sensitivity of the HRTFs to the averaging areas. On the other hand, it is noted that the second ear case is creating a
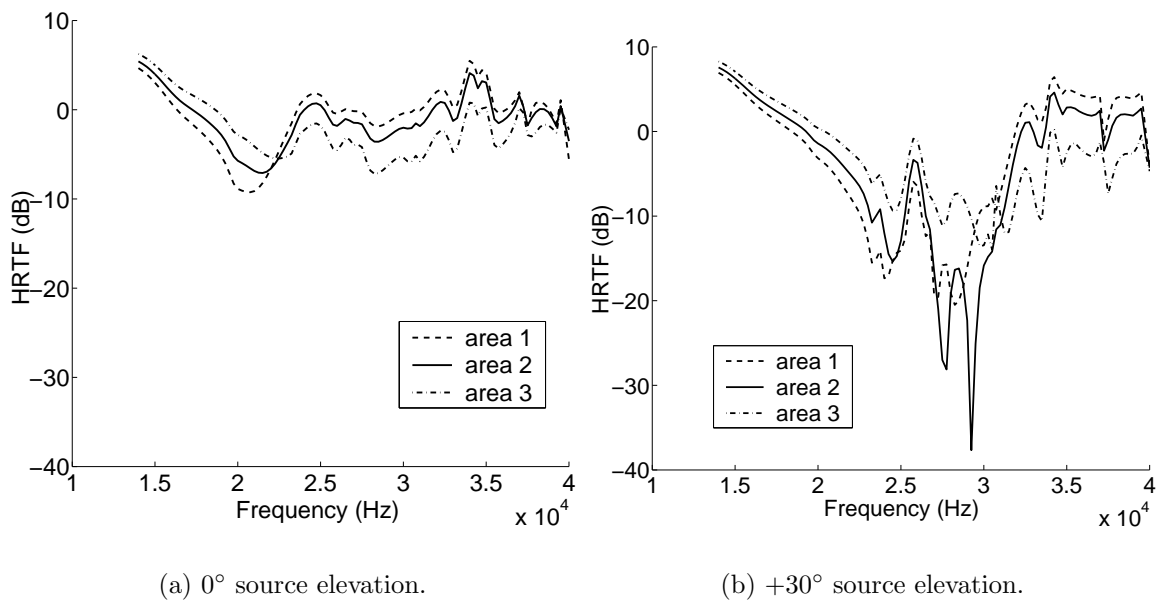
14

(a) 0° source elevation.

(b) +30° source elevation.

FIG. 3. HRTF sensitivity to measurement area for the first ear model. Source located 0.3 m from head (no torso present). Two elevations: 0° and 30°. HRTF computed from pressure averaged over three different areas shown in Figure 2.

pinna notch with a wavelength on the order of the height of the pinna. Thus it seems that when there is an obvious geometric driver for the scattering of the incident field leading to the creation of the notch, the averaging area is less important.

The result of the pinna base area study indicates that the HRTF can be sensitive to the location and extent of the measurement device. This is supported by the measurements described in (Maki and Furukawa, 2005). The results presented in the following sections were all obtained by using the medium size area (i.e. "area 2").

4.2. HRTF for gerbil in the free field

The influence of the gerbil torso on the free-field HRTF was investigated using the first ear model and averaging area 2. The notch position was not affected by the presence of the torso, but the notch was slightly shallower when the torso was

(a) 0° source elevation.   (b) +30° source elevation.
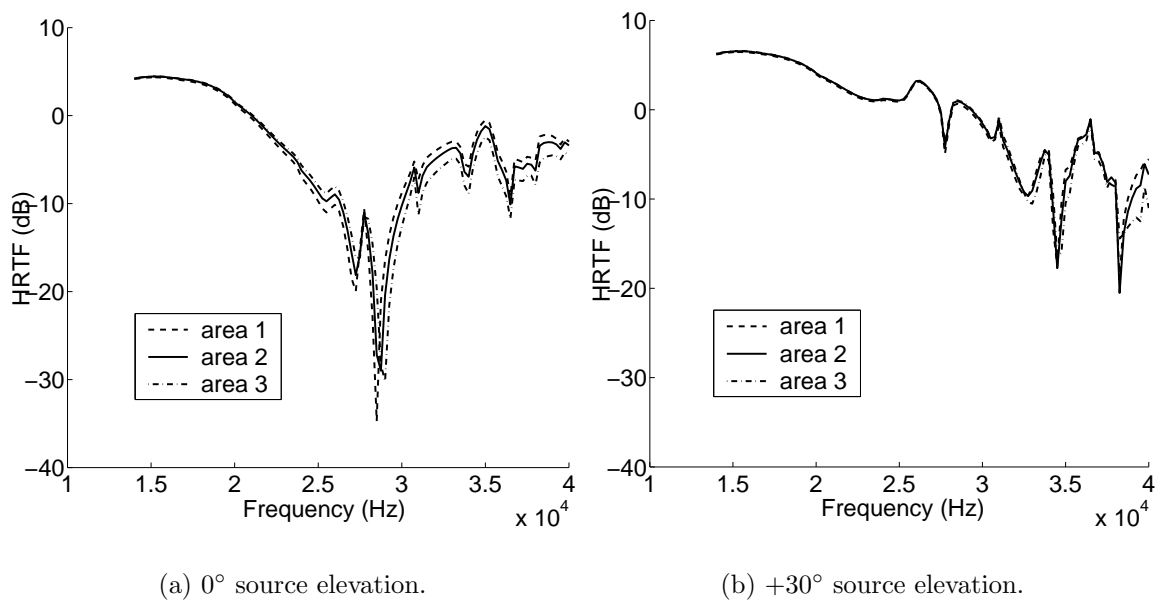
FIG. 4. HRTF sensitivity to measurement area second ear model. Source located 0.3 m from head (no torso present). Two elevations: 0° and 30°. HRTF computed from pressure averaged over three different areas shown in Figure 2.

present. It was thus determined that the HRTF could be studied using just the head of the model gerbil; and as such, the results in this section were obtained for only the gerbil head model.

Figure 5 shows the HRTFs obtained for the two ear geometries at various source distances. The source is directly in front of the head in the median plane and the head model is completely symmetric. A notch is present at approximately 22 kHz and 28 kHz for the first and second ear geometries respectively, and the effect of the source distance on the HRTF is almost negligible. The small discontinuity seen at 14 kHz results from the two different grids used for the low and high frequencies.

Figure 6(a) shows the HRTFs for various source elevations for the first ear model. The source is moved from −30° to +90° in 30° steps while keeping the distance from the head center fixed at 0.3 m. For clarity, the results for each source elevation
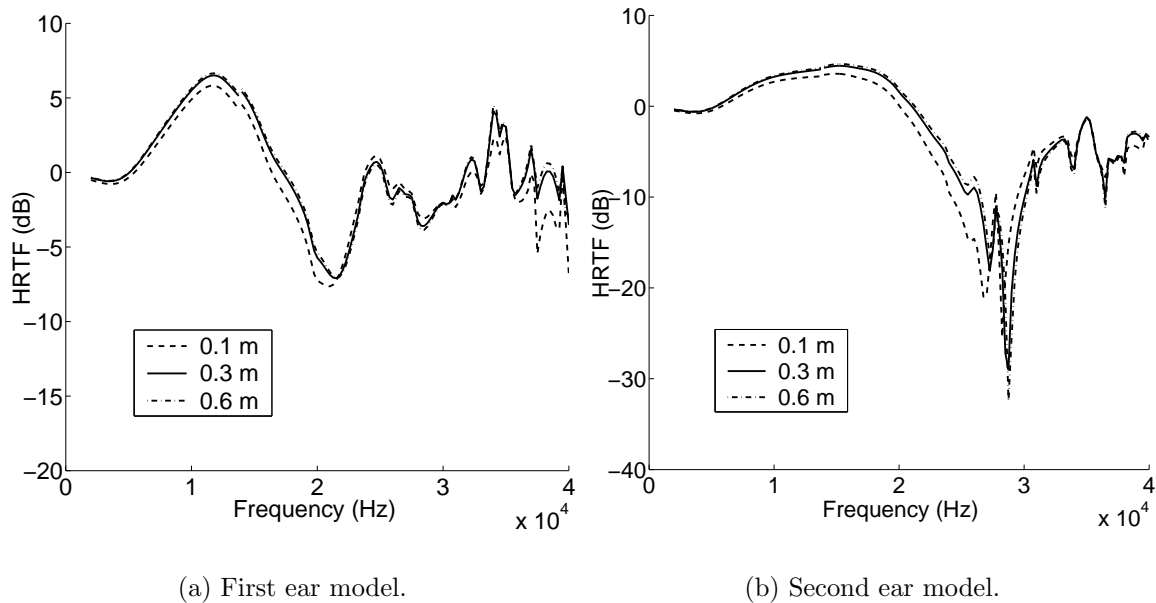
(a) First ear model.
(b) Second ear model.

FIG. 5. Effect of source distance on the HRTF for the two ear models. Source elevation 0°, head alone, "area 2" for average.

have been shifted by 10 dB. The notches are indicated by arrows in the figure. For most elevations, the notch is very clear, but in the 30° elevation case there is some ambiguity.

Three source elevations were considered for the second ear model. The resulting HTRFs are shown in Figure 6(b). For this ear model the notches at the -30° and 0° elevations are much clearer, however at 30° the spurious roots make notch identification more difficult.

Quantitative comparison with the experimental data requires one to consider the directional transfer function (DTF) of the measured data because the notches are not very clear in the measured HRTF. The DTF for M source locations at each frequency is given by

$$DTF = 20\,Log\left(\frac{\hat{p}}{p^I}\right) - 20\,Log\left(\frac{\sum_{i=1}^{M}\hat{p}_i}{Mp^I}\right), \tag{3}$$

17

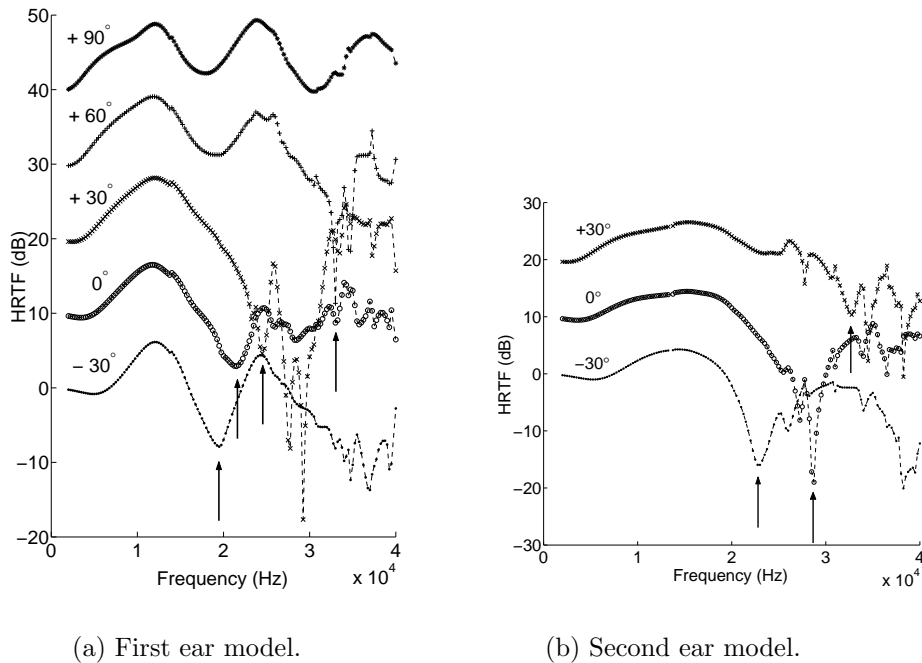(a) First ear model. (b) Second ear model.

FIG. 6. Effect of source elevation on the HRTF for a gerbil in free-space. Source distance 0.3 m head alone, "area 2" for average.

where the summation is used to compute the average response (total pressure amplitude) due to the M different source locations. Maki and Furukawa (2005) contend that the HRTF contains information dependent upon the position of the measurement device in the ear canal and that the DTF removes these features. Maki *et al* averaged the HRTFs from 937 source locations with varying elevation and azimuth angles to obtain the DTF. In our model, the ear canal is not present and the notches are apparent in the HRTF although there is a gain in the low frequency range that is independent of source location and as such would not appear in a DTF of the computed results.

Maki *et al* measured the DTF of the right and left ears of several gerbils. They show the DTF results for two gerbils that they denote as No. 521 and No. 1020.

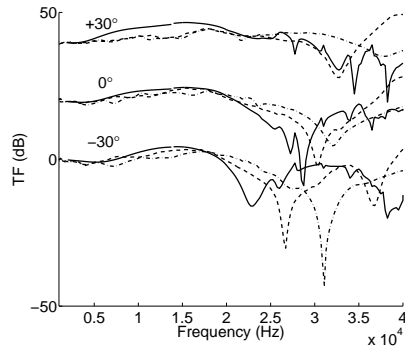Figure 7 shows the DTF for the right ear of No. 521 and the left ear of No. 1020

FIG. 7. Comparison of experimental DTF and computational HRTF at 3 elevations for gerbil with second ear model to experimental results of Maki. Solid line - numerical results, dashed line - right ear of the No. 521 gerbil, dash dot line - left ear of the No. 1020 gerbil.

compared to the computed results for the second ear model. The results of the three elevations are offset by 20 dB for easier comparison. At low frequency, where the HRTF does not depend on the detail of the pinna, the experimental and computational results match matches extremely well for the -30° and 0° elevations. Overall, the computed results match the results for the gerbil No. 521 better. The computed notch frequency for -30° is off by 5 kHz, for 0° it is off by 2 kHz, and and for -30° it matches well. The trend found experimentally of reduced notch depth with increasing elevation is not matched perfectly. In summary, the HRTF for the simulated head and pinna has a notch frequency that is more sensitive to elevation and a notch depth that is less sensative to elevation than that measured for the No. 521 gerbil ear. Overall however, the results give a good fit to the empirical data especially given the crudeness of the geometric model used in the computation.
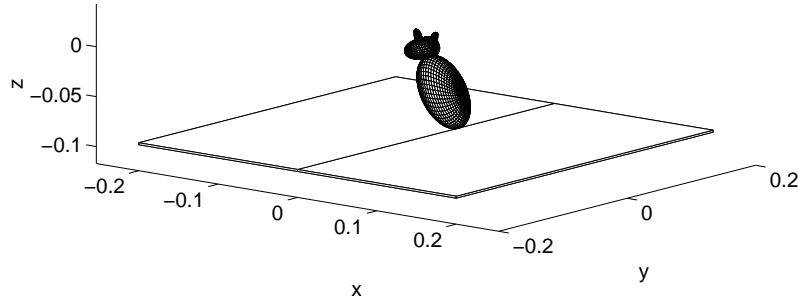
FIG. 8. Gerbil with model floor.

4.3. Floor Effect on Gerbil BETF

Two geometries were used to model the effect of the floor on the gerbil BETF. First a thin finite box ($0.4\ m \times 0.4\ m \times 0.001\ m$) with the gerbil geometry centered on the box as shown in Figure 8 was considered. Second, an image gerbil was created to simulate an infinite floor. All of the results in this section were obtained for the gerbil geometry that includes the torso. Figure 9 shows the BETF computed using the two floor models (thin box and image gerbil) when the source is at $0°$ elevation and a distance of $0.1\ m$ from the gerbil head. The BETF shown is referenced to the free-space incident pressure field.

In the low frequency range, it is clear that the frequency notches are related to interference between the wave coming directly from the source (path A in Figure 10) and the wave reflected by the floor (path B in Figure 10). For frequences where the difference between the two path lengths is an odd multiple of half of the wave length, the wave coming from the source and the one reflected by the floor cancel. Overlayed on the computed BETFs in Figure 9 is a curve denoted as the ray method curve.
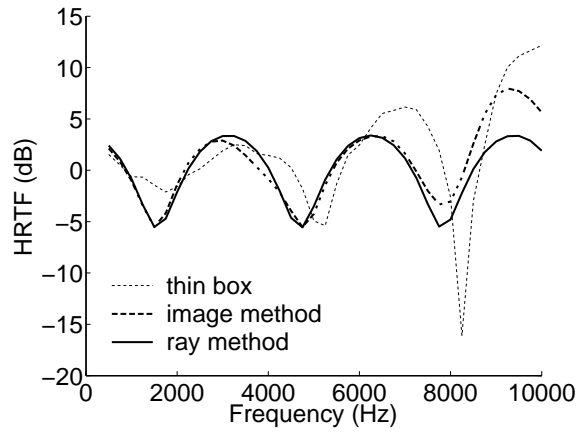
20

FIG. 9. BETF for gerbil head and torso (first ear model) on a thin finite box and on an infinite floor. Source at 0.1 m and 0° elevation measured from head. BETF computed using free-space source pressure as reference. Also, total incident pressure for floor alone (no gerbil) computed using the ray method normalized by the free-space source pressure.

This curve represents the total incident field at the base of the pinna (without the gerbil present). I.e. the total pressure at the base of the pinna, $\hat{p}$, that appears in the definition of the BETF in Equation (1), which was obtained by analytically evaluating the influence of the originating source and the reflections from the floor without the gerbil present. Thus, differences between the ray method and the computed results highlight the effect of the gerbils presence on the total pressure field at the base of the pinna.
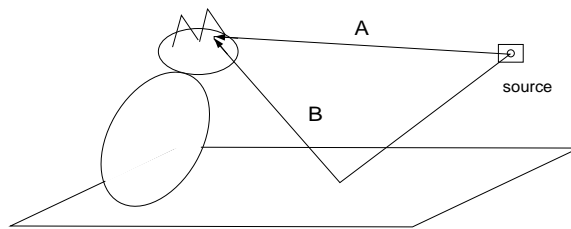

FIG. 10. Ray method paths.

The geometric lengths in this problem are reflected in the BETF. The finite box has a dominant length of 0.2 m from the gerbil to its edges. This translates to a

Grace

frequency of 1700 Hz. Figure 9 shows that the thin box and image methods differ the most at multiples of 1700 Hz, emphasizing the importance of the box edge scattering in the BETF. The distance of the gerbil ear from the floor is 0.095 m, which relates to a frequency of 3580 Hz. At frequencies below 8 kHz, the difference between the computation that includes the gerbil and the computation for just the floor scattering is greatest at multiples of this frequency. Past a frequency of roughly 8 kHz, when other geometric details such as the head size become much more important, all of the methods diverge.

Originally, the thin box model was developed to simulate the finite extent floor that was used in experiment. However, it is computationally less intensive to study the impact of source distance for example if one uses the infinite floor model (image method) because of the increased grid size that accompanies discretizing a thin box with large extent. Because the main differences between the thin box results and the infinite floor results arise at frequencies associated with the length scale related to the finite floor, and the salient features of the comb-filtering are captured with both methods, the results reported in the rest of this section were obtained using the infinite floor model. A solid wall boundary condition was used here to match the experimental setup of Maki *et al.* (2003a). In nature, the gerbil's environment is made of uneven sand covered ground. The results in the limit of complete absorption will correspond to the free-field results discussed in the previous section. In the limit of complete reflection, results will correspond to the results reported in this section. The image method used to obtain the results in this section cannot be used if one needs to model an uneven ground, or ground with inhomogeneities. Instead, the
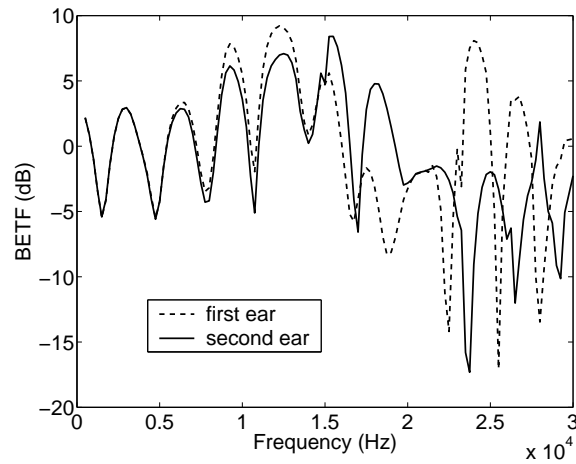
22

FIG. 11. BETFs for the gerbil on an infinite floor. First and second ear models. Source at 0° elevation and 0.1 m distance from the head. BETF normalized by the free-space incident pressure field.

more computationally intensive thin box method would have to be employed where

the ground is discretized as a thin box with the salient geometric features.
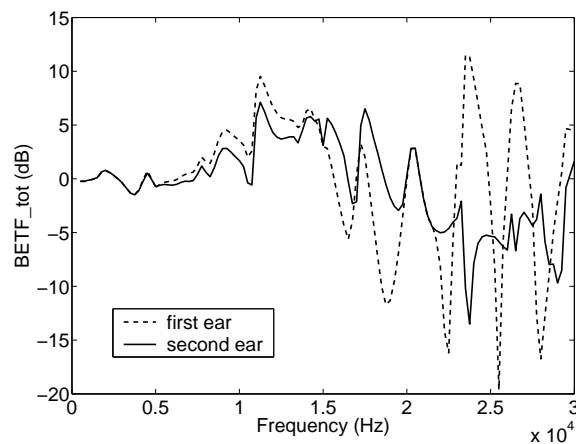

FIG. 12. BETFs for the gerbil on an infinite floor. First and second ear models. Source at 0° elevation and 0.1 m distance from the head. BETF normalized by the total incident pressure field.

Figure 11 shows the BETFs for the gerbil on a solid floor with the two different

ear geometries. The source is located 0.1 m from the head with 0° elevation. The

BETF is normalized by the free-field incident pressure and as such the influence

of the environmental cue (the floor) is clear. The results agree with the results

reported by Maki *et al.* (2003b) because they are dominated by the environmental input. As pointed out by Maki *et al*, these environmentally produced notches justify the neurological behavior of the gerbil DCN that shows excitatory responses to best frequency tones as low as 1 kHz.

If one is interested in the importance of the interaction between the environmental cues and the gerbil geometry, it is better to normalize the total pressure at the base of the pinna by the total incident pressure (i.e. the pressure field due to the environment at the pinna location when only the gerbil is absent). When this normalization factor is used, the comb filtering is factored out. What appears are the variations due to various geometrical length scales related to the gerbil. For instance, Figure 12 shows the BETFs with this normalization for the gerbil on an infinite floor (image method). The length scales associated with the elliptical head geometry are 0.033 m and 0.02 m. These lengths translate to frequencies of 10.3 kHz and 17 kHz. The BETF's for the two ear geometries begin to deviate at 10.3 kHz, and further deviate at 17 kHz. Nearer to the frequencies associated with the pinna length scales the largest deviations are seen. (The height of the pinna for the two ear models corresponds to a frequency of 26 kHz.)

The augmentation of the total pressure field at the pinna due to the presence of the listener is even more pronouned when comparing the BETFs for sources at different elevations. The BETFs for the gerbil with the second ear geometry produced by sources at a radial distance of 0.3 m from the center of the head at three elevations are displayed in Figure 13. Both normalization methods are shown. The comb-filtering effect is again very clear when the free-space incident field is used for the

normalization. The results highlight the fact that the reflected energy from the floor can provide source elevation cues.
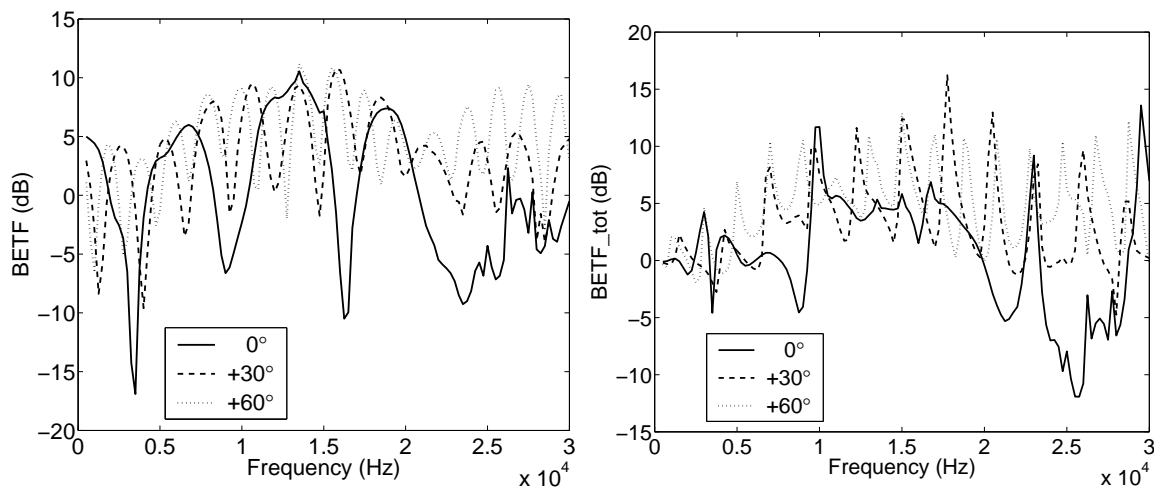
(a) Normalized by the free-field incident pressure.

(b) Normalized by the total incident pressure.

FIG. 13. BETFs for the gerbil on an infinite floor. Second ear model. Sources at 0.3 m distance from the head and 0°, 30°, 60°. BETF normalized by the free-field incident pressure field (a), and the total incident pressure field (b).

When the normalization is performed using the total incident field, it becomes clear that not only does the reflected energy provide potential elevation cues but that its effect is strengthened by its coupling to various geometrical scales of the listener. For instance, the notch seen at 9 kHz in the zero elevation case coincides with the wave whose length is equal to half the distance between the floor and the gerbil's chin. When the source is moved from a distance of 0.3 m to 0.1 m from the gerbil's head, it is the -30° elevation whose reflection pattern enhances this feature and produces a notch at 9 kHz while the zero elevation case does not exhibit such behavior as seen in Fig. 14.

Because the environmental cues from the floor (in isolation) are dominated by the
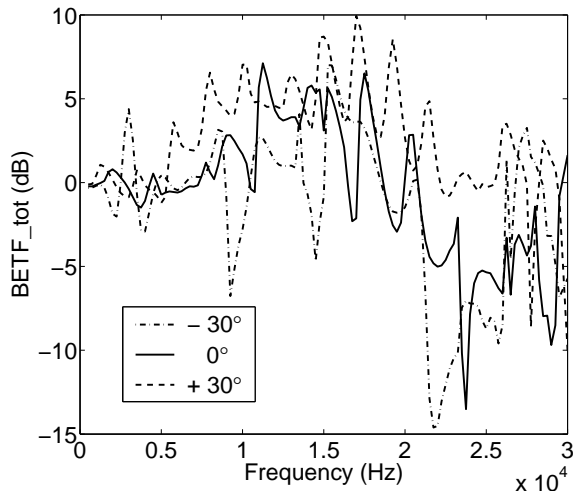
FIG. 14. BETFs for the gerbil on an infinite floor. Second ear model. Sources at 0.1 m distance from the head and -30°, 0°, 30°. BETF normalized by the total incident pressure field.

differences in pathlength between direct and reflected sound (see Fig. 10), it is easy to determine the locus of source locations that provide the same environmental cue. Figure 15 shows the isolines for sources in the median plane and a gerbil ear located 0.01 m off center and 0.095 m above the ground. The BETF's for five sources along one isoline are shown in Figure 16. The five sources are noted on Figure 15. The BETFs are shown normalized by both the free-field incident pressure and the total incident pressure. While the sources produce the same incident pressure pattern, the BETFs are not identical (even at the low frequencies) for the three sources. The low-frequency notches are deeper for sources at higher elevation. The notch depth difference is highlighted when one computes the BETF using the total incident field as the reference pressure. This highlights an even more subtle feature than displayed in the previous elevation study. Here the differences are not easily associated with specific geometric features.

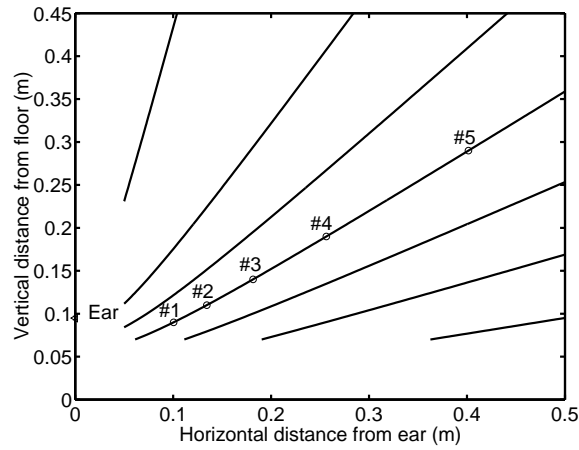These subtle differences that appear in the BETF's for isosources in the median

FIG. 15. Isolines of source locations in the median plane that produce the same environmental cue for a gerbil on an infinite floor. Location of the gerbil ear shown on the left axis. Location of sources used for BETF comparison noted.

plan (selected at distances and elevations such that they produce that same comb-filtering effect) and the profound differences that appear for sources in the median plane with equal radial position cannot be captured if one only considers the comb-filtering contribution of the ground plane. Indeed this work shows that the interplay between the listener and the ground plane is critical.

In the psychoacoustics literature, reflected energy from environmental obstacles is often discussed as if its main effect is to interfere with and distort directional information, such as information conveyed by the interaural and spectral spatial cues in the signals reaching the ears (Shinn-Cunningham *et al.*, 2005; Hartmann *et al.*, 2005). In contrast with these past results, this study shows that the systematic alterations in the spectral content of the signals reaching the gerbil's ears (either in conjunction with or in leiu of the enhanced geometrical features) caused by floor reflections may provide information about source elevation. Indeed for the gerbil, rather than distorting the HRTF cues that are thought important for localization,
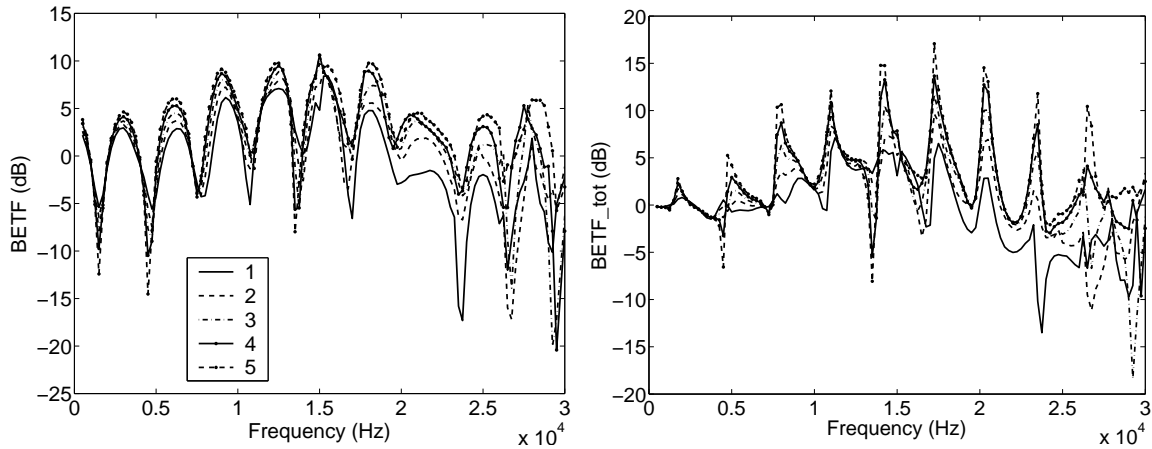
(a) Normalized by the free-field incident pressure.

(b) Normalized by the total incident pressure.

FIG. 16. BETFs for the gerbil with the second ear model on an infinite floor from sources that provide the same environmental cue. Source locations shown in previous figure. First normalization using free-field incident pressure. Second normalization using total incident pressure.

the computations show that the floor reflection provides an independent cue for source direction in the median plane and this cue is dependent upon interactions that can be captured via a simulation based on BEM but would not be captured by a simple ray-tracing approach. This gives further support for the importance of simulation tools that are able to incorporate both the listener and environmental effects into the acoustic scattering model.

5. SUMMARY

A frequency domain boundary element method was used to computationally model the gerbil's binaural environmental transfer function (BETF) for sources located in the median plane. The CHIEF method was implemented to regularize the spurious root phenomenon and the interior points were chosen such that they coin-

cided with the location of the maxima in the velocity potential when not regularized. However, a more robust regularization method is recommended for future use because of the poor performance of the CHIEF method at very high frequency.

A simplified gerbil geometry was created based on anatomical data from gerbils used in empirical experiments and the gerbil was treated as a rigid scatterer. These empirical results provide the validation data for the current study. The ability to both take advantage of the symmetry in the problem (i.e. reduce the number of unknowns) and implement parallel processing lead to reasonable runtimes for simulations spanning a wide range of source frequencies (1- 30 kHz) and using surface discretizations of at least 10 points per wave. In most cases 15 or 20 points per wave were used.

Although the gerbil model is very simple, the computations capture notch characteristics that are found experimentally, namely: a) that the BETF consists of multiple notches starting in the range of 1 kHz when the gerbil is on a solid surface, but the HRTF for the free-field contains a low number of notches (often just one) in the ultrasonic range for the free-field condition, b) notch frequency and depth are dependent on pinna geometry for the free-field case but are only slightly dependent on gross anatomical length scales when the surface is present, c) source distance (beyond the very near-field) does not influence the free-field HRTF, but is a critical parameter for the BETF d) an increase in source elevation leads to an increase in the notch frequency for the free-field condition, a decrease in the spacing between notches when the surface is present, and

Notches that appear in the low frequency part of the spectrum when the gerbil

is on a solid surface, e.g. $< 10kHz$ for the second ear model, are highly dependent upon the interference pattern set up by the reflections from the surface. However, the augmentation of the comb filtering due to the gerbil geometry is present at the lower frequencies. This contribution of the gerbil's anatomy to the BETF for the case of a gerbil standing on a solid surface is best highlighted using the *total* incident pressure as the normalization factor in the BETF.

The results reported here thus indicate that reflected energy can provide information about source elevation as well as source distance. Moreover, the environmental cues are influenced by the listener geometry and its interactions with the environment and thus cannot simply be superimposed on an HRTF to produce the BETF.

The BEM has been shown to be a powerful tool for predicting the BETF of gerbils in real environments. This tool can now be used to study the effect of environmental inhomogeneities, environmental and animal fur acoustic absorption, and predator sound cues.

6. ACKNOWLEDGEMENTS

References

L. S. Blackford, J. Choi, A. Cleary, E. D'Azevedo, J. Demmel, I. Dhillon, J. Dongarra, S. Hammarling, G. Henry, A. Petitet, K. Stanley, D. Walker, and R. C. Whaley, *ScaLAPACK Users Guide*, Philadelphia (1997).

J. Blauert, *The Psychophysics of Human Sound Localization* (Cambridge: MIT Press) (1993).

J. Fels, P. Buthmann, and M. Vorlander, Head-Related Transfre Functions of Children. Acta Acustica United with Acustica **90** (2004) 918–927.

W. M. Hartmann, B. Rakerd, and A. Koller, Binaural coherence in rooms. Acustica united with Acta Acustica **91**(3) (2005) 451–62.

U. Iemma, BEM simulation of woodwind musical instruments. in *The 7th International Congress on Sound and Vibration* (Garmisch-Partenkirchen, Germany) (2000).

Y. Kahana, Numerical Modelling of the Head Related Transfer Function. Ph.D. thesis, University of Southampton (2000).

B. Katz, Measuraments and Calculation of Individual Head-Related Transfer Function Using a Boundary Element Model Including the Measurements and Effect of Skin and Hair Impedence. Ph.D. thesis, The Pennsylvania State University (1998).

B. Katz, Boundary element method calculation of individual head-related transfer function. I. Rigid model calculation. Journal of the Acoustical Society of America **110**(5) (2001a) 2440–2448.

B. Katz, Boundary element method calculation of individual head-related transfer function. II. Impedance effects and comparisons to real measurements. Journal of the Acoustical Society of America **110**(5) (2001b) 2449–2455.

K. Maki and S. Furukawa, Acoustical cues for sound localization by the Mongolian gerbil, Meriones unguicalatus. Journal o the Acoustical Society of America **118**(2) (2005) 872–886.

K. Maki, S. Furukawa, and T. Hirahara, Acoustical cues for sound localization by gerbils in an ecologically realistic environment. Association for Research in Otolaryngology (2003a), aRO abstract and poster 332.

K. Maki, S. Furukawa, and T. Hirahara, Head-related transfer functions of the Mongolian gerbil in the median plane. Acoustical Science and Technology **24**(5) (2003b) 330–332.

A. Musicant, J. Chan, and J. Hind, Direction-dependent spectral properties of cat external ear: New data and cross-species comparisons. Journal of the Acoustical Society of America **87**(2) (1990) 757–781.

Y. Naka, Numerical methods for solving the wave equation in large enclosures with application to room acoustics. Ph.D. thesis, Boston University, Boston, MA (2006).

M. Otani and S. Ise, A fast calculation method of the head-related transfer functions for multiple source points based on the boundary element method. Acoustical Science and Technology **24**(5) (2003) 259–266.

J. E. Parsons, E. Lim, and H. F. Voigt, Type III units in the gerbil dorsal cochlear

nucleus may be spectral notch detectors. Annals of Biomedical Engineering **29** (2001) 887–896.

E. Quaranta, Application of the boundary element method to computation of the head-related transfer function for gerbils. Master's thesis, Boston University, Boston, MA (May 2004).

B. Rakerd and W. M. Hartmann, Localization of sound in rooms, II: The effect of a single reflecting surface. Journal of the Acoustical Society of America **78**(2) (1985) 524–533.

V. C. Raykar, R. Duraiswami, and B. Yegnanarayana, Extracting the frequencies of the pinna spectral notches in measured head related impuse responses. Journal of the Acoustical Society of America **118**(1) (2005) 364–374.

J. Rice, B. May, J. Spirou, and E. Young, Direction-dependent spectral cues for sound localization. Hearing Research **58** (1992) 132–152.

B. G. Shinn-Cunningham, N. Kopco, and T. J. Martin, Localizing nearby sound sources in a classroom: Binaural room impulse responses. Journal of the Acoustical Society of America **117**(5) (2005) 3100–3115.

M. Snir, S. W. Otto, S. Huss-Lederman, D. W. Walker, and J. Dongarra, *MPI: The Complete Reference* (MIT Press, Cambridge, MA) (1995).

M. Spezio, C. Keller, and T. Takahashi, Head-related transfer functions of the Rhesus monkey. Hearing Research **144** (2000) 73–88.

G. A. Spirou and E. D. Young, Organization of dorsal cochlear nucleus type IV Unit response maps and their relationship to activation by bandlimited noise. Journal of Neurophysiology **66** (1991) 1750–1768.

L. Xu and J. Middlebrooks, Individual differences in external-ear transfer functions of cats. Journal of the Acoustical Society of America **107** (1980) 1451–1459.

E. Young, J. Rice, and S. Tong, Effects of pinna position on head-related transfer functions in the cat. Journal of the Acoustical Society of America **99**(5) (1996) 3064–3076.

E. D. Young, G. A. Spirou, J. J. Rice, and H. F. Voigt, Neural organization and responses to complex stimuli in the dorsal cochlear nucleus. Philosophical Transactions of the Royal Society (London) **336** (1992) 407–413.